



CHRONOLOGY OF CONSTRUCTION AND OCCUPATIONAL PHASES OF NAWAMIS TOMBS, SINAI BASED ON OSL DATING

IOANNIS LIRITZIS¹, NIKOLAOS ZACHARIAS², FAHAD AL-OTAIBI³, IOANNIS ILIOPOULOS⁴,
CHRISTOS KATAGAS⁴ and MOSSALAM SHALTOUT⁵

¹King Saud University, Riyadh, Saudi Arabia & Lab of Archaeometry, Dept of Mediterranean Studies,
University of the Aegean, Rhodes, Greece

²Laboratory of Archaeometry, Department of History, Archaeology and Cultural Resources Management,
University of the Peloponnese, 24133 Kalamata, Greece

³King Saud University, Dept of History, Riyadh, Saudi Arabia

⁴Department of Geology, University of Patras, 26504 Rio, Greece

⁵National Research Institute of Astronomy and Geophysics (NRIAG), Helwan, Cairo, Egypt

Received 8 March 2016

Accepted 19 September 2016

Abstract The *Nawamis* are sandstone-built circular structures, located at several sites across Southern Sinai, Egypt. They are thought to be family tombs, created by the nomadic people that inhabited the area. Archaeological age estimates fall within the Early to Late Bronze Age. Here an interesting suite of nine OSL dates of three stone pieces has been resulted, from two *Nawamis* at Gebel Gunna and Ain Khodra fields. Single aliquot regeneration OSL of quartz grains provided the accumulated dose. XRD was used to identify mineralogy of several tombs. Based on the estimated luminescence ages a time span from Early and late Bronze ages is obtained, while some possible later activity, due to partial (re)construction or reuse of tombs, was detected.

Keywords: Nawamis, surface luminescence dating, Bronze Age Levant, SAR-OSL, XRD.

1. INTRODUCTION

The *Nawamis* are stone-built circular structures, located at several sites across Southern Sinai (**Fig. 1**).

Earlier rescue excavations at Gebel Gunna have reported skeletons, lithic axes, scrappers, some copper bronze, grinding stones, hammer stones, beads, shells, with much debitage and debris.

According to initial excavators (Bar-Yosef *et al.*, 1977, 1986) *Nawamis* appear to be family tombs, made by nomads, that inhabited the area. The age inferred by ceramic and artifact typology, as well as, C14 of charcoal

assigns them to a range of Early Bronze Age (EB) I, II mainly EB II. (*ca.* 2700 B.C.), though Late Bronze age (1550–1200 BC) artifacts are also reported. Reuse of tombs evidenced from diagnosed finds has been noticed with later Roman-Byzantine period, even with some Bedouin burials of unknown age- all of which though may have been subjected to unnoticeable repairs. Primary and secondary burials were mixed and disturbed in historic times (Bar-Yosef *et al.*, 1977, 1986).

There are approximately 1000 *Nawamis* in Sinai, some of them in very good condition, others almost destroyed (Herskovitz *et al.*, 1985; Bar-Yosef *et al.*, 1983).

All *Nawamis* are characterized by the same have same rounded plan, 3 to 6 meters in diameter and about 2 meters height. They are double-walled structures, built on local rocks, usually sandstones. The outer wall is standing upright and the inner wall rises in an arch and forms a

Corresponding author: I. Liritzis
e-mail: liritzis@Rhodes.Aegean.gr

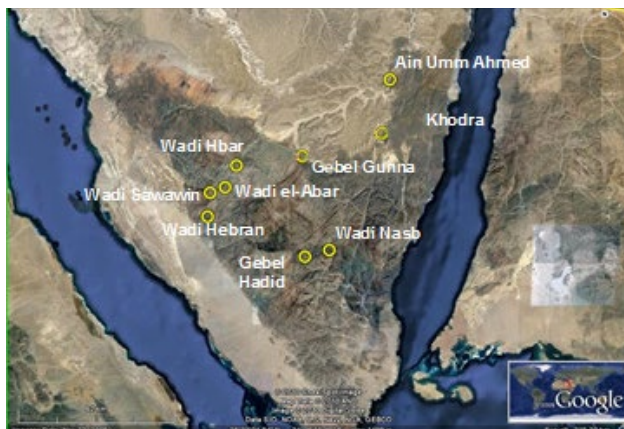


Fig. 1. Location of Nawamis in the Sinai Peninsula for the sites of Gebel Gunna and Ain Khodra.

corbelled roof lidded by a larger slab. They were built by rough rectangular slabs fit one to another and in a simple manner of construction. The entrances are small corridors made by one or two standing slabs, that remained in place despite later collapse of some of them. In the preserved ones their entrances appear to face west.

Optically stimulated luminescence dating (OSL) followed surface luminescence dating procedures of Liritzis *et al.* (2013a) to date for first time two *Nawamis*, in Gebel Gunna and Ain Khodra areas, to investigate construction or re-use of these nomadic tombs.

The geolithology of the area comprises of sandstones intercalating with various carbonate rocks and shales, which belong to the Mahla Formation (Wanas, 2011). These are unconformably underlain by low-lying sandstone of the Naqus formation, which together with the granitic rocks of the Precambrian basement form a pronounced relief reaching about 1200 meters above sea level.

2. LUMINESCENCE DATING OF WALLS: THE RATIONALE

The luminescence technique employed in this study has been introduced during the 90's (Liritzis, 1994), and thereafter tested and published elsewhere (Huntley and Richards, 1997; Habermann *et al.*, 2000; Morgenstein *et al.*, 2003; Greilich *et al.*, 2005), with an overview of the surface dating reported later in this journal by Liritzis (2011), followed by successfully applied case studies (Sohbati, 2013; Liritzis *et al.*, 2013a, 2013b, 2015; Liritzis and Vafiadou, 2014) or reported in review articles about the use of OSL in different materials (Roberts *et al.*, 2015). In masonry it involves dating the inter-block surfaces of building stones which relies on the optically sensitive electron traps responsible for OSL light in the surface layer of the carved rock, having been bleached by sunlight, prior to the blocks being incorporated into the structure. The sunlight bleaching of quartz in sandstone

surfaces is in fact fast (Liritzis *et al.*, 2010b; Liritzis and Vafiadou, 2014). Subsequently, the slabs exposed to sunlight are moved in the appropriate position of the structure and overlaid by another block. From the moment that any surface is no longer exposed to sunlight and put in firm contact (with or without mortar), the optically sensitive electron traps are filled by electrons produced by the ionization caused from nuclear radiation of natural uranium, thorium, potassium, rubidium and cosmic radiation. These isotopes are present in the rock slabs and the soil surrounding the sampling point. Thus, the age can be given by Eq. 2.1:

$$\text{Age} = \text{ED (Gy)} / \text{DR (mGy/yr)} \quad (2.1)$$

The equivalent dose (ED, in Grays, Gy) is measured by (OSL) following standard procedures of SAR (Murray and Wintle 2000; Greilich *et al.*, 2005; Liritzis *et al.*, 2010b).

The annual dose rate (DR, in mGrays per year) denotes the radiation dose accumulated in a year. It is comprised of the three-radiation dose components (alpha, beta and gamma radiation) derived from the natural radioisotopes of uranium (U-238), thorium (Th-232), potassium (K-40), and rubidium (Rb-87), of the sample itself and the surrounding environment, and includes cosmic-rays (Aitken, 1985).

3. SAMPLING

With the aid of a chisel and a hammer samples were detached from firm contacts and swiftly covered to avoid sun exposure. In fact care was taken when removing the samples to avoid light: sampling was made during the sunset working under an *in situ* mini tent to light deprive, they were gently chipped and when loose while still in original position in the wall and covered by mortar, were gently removed being wrapped by black plastic bags, while adherent sand on the contact of the two cobbles was collected too (Liritzis *et al.*, 2010, 2015; Liritzis 2010). Surficial pieces of rock about 6–8 cm² and at least 0.5 cm thick were detached. (Fig. 2). By adhering to this protocol, we insure that the samples collected in the field were not exposed to light.

At Gebel Gunna 6 inside the rectangular structure wall sampling was made about 60 cm above the bedrock floor, and from Ain Khodra 8 both samples came from the external wall at a height of about 1.00 m above bedrock ground (Fig. 3). Nine sub-samples were processed from three removed pieces; one piece derived from Gebel Gunna tomb (the GG6 with three sub-samples), and two pieces from Ain Khodra (AK8.1, with two sub-samples, and AK8.2 with four sub-samples from both surface faces).

A surface layer of about 50 μm (measured by a micrometer), which included organic material, dust, and adherent contamination, was removed from the inner surface by briefly inserting it in dilute hydrochloric acid



Fig. 2. Actual sample obtained from the structures, wrapped in opaque bag to avoid sunlight. (scale: longer length ~4 cm). Here the opposite side is shown that is of no interest to dating for clarity of sample size and shape.

HCl acid (10 wt%) and rinsed with running water. Subsequently, a thin layer of surface polymineral powder was acquired by gently scraping the inter block surface to a depth of less than 0.5 mm (making a series of readings with a micrometer) and transferred to an acetone bath where grains were collected, washed in dilute acetic acid (5 wt%) for 1 min, and dried. Medium sized grains of sandstone were sieved to a diameter of 50–110 μm , washed in HF for 45 min to remove a layer of ~25 μm to avoid alpha particle dose rate contribution, prior to OSL measurements.

Sub-samples of the ancient carved surface were taken (by dividing the surface into sizeable parts to acquire sufficient quantity powder for SAR and tests), to reassure regions of interest (ROI) that were not subjected to possible effect of friction (from past earthquake) of two stones in contact. Such an event destroys originally bleached surface layer and provides powder of deeper surface layers not bleached and thus inhere geological luminescence. Where appropriate, two or three sub ROI were selected (see Fig. 6) (in fact, two contact surfaces do not touch each other completely, but there exist sub-areas at the millimeter level of voids; those sub-areas of interest are searched for obtaining consistent equivalent doses, with others, usually high values, as outliers, discarded regarded of geological origin).

4. INSTRUMENTATION & MEASUREMENTS

Prior to any sample preparation the mineralogy was checked by XRD, then equivalent dose and dose rates were measured. XRD analyses were performed on the same samples (Ain Khodra 8, Gebel Gunna 6) that were used for dating, as well as, from other rock types of local environment shown in Table 1. Stone was visually similar but mineralogical characterization was decided to be a necessity in order to detect differentiations that potentially point to the exploitations of different quarries and/or

different chronological periods of use; checking even small variations was of interest and as a future reference too.

XRD analysis

A small aliquot from the samples was used in order to determine the mineralogical composition by means of X-ray powder diffraction (XRD) analysis. Samples were firstly dried in a laboratory oven at 110°C for 24 h and then grinded in a vibration disc mill using an agate grinding set. The samples were then analysed in a Bruker D8 Advance X-Ray diffractometer, with Ni filtered CuK α radiation, operating at 40 kV/40 mA, in the Laboratory of Mineral and Rock Research of the Department of Geology at the University of Patras, Greece. The scanning area covered the interval 2°–70° 2 θ , with a scanning angle step of 0.015° 2 θ and a time step of 0.1 s (Iliopoulos *et al.*, 2011). The interpretation of the acquired diffractograms and mineral identification was performed using DIFFRACplus EVA software (Bruker-AXS, Madison, WI, USA) based on the International Centre for Diffraction Data Powder Diffraction File (2006). Representative rocks from several tombs are examined. The rock was identified as sandstone with predominant quartz, few kaolinite and only traces of other minerals such as calcite, hematite, gypsum and muscovite (Table 1 and Fig. 4). Lazurite was only identified in the sample from Gebel Gunna 2 (Airp2). This blue colored mineral is the essential ingredient of lapis lazuli, a precious stone well known in prehistoric times, which was widely imported from Afganistan to Egypt. The composite XRD diagram of Fig. 4 illustrates well the quartz predominance in all samples.

Table 1. Mineralogical composition of the analyzed samples as determined through XRD analysis. Airp stands for rocks around airport (+: dominant; x: present; tr: traces; -: not determined).

Sample ID	quartz	kaolinite	calcite	muscovite	hematite	lazurite	gypsum
Airp 1	+	x	x	-	-	-	tr
Airp 2	+	x	tr	tr	-	tr	-
Airp 3	+	x	x	-	-	-	-
Airp 5	+	x	tr	-	-	-	-
Airp 7	+	x	-	-	x	-	-
Airp 14	+	x	x	-	-	-	tr
Airp 6 (Ain Khodra 8.1)	+	x	tr	-	-	-	-
Gebel Gunna 6	+	x	-	tr	tr	-	-

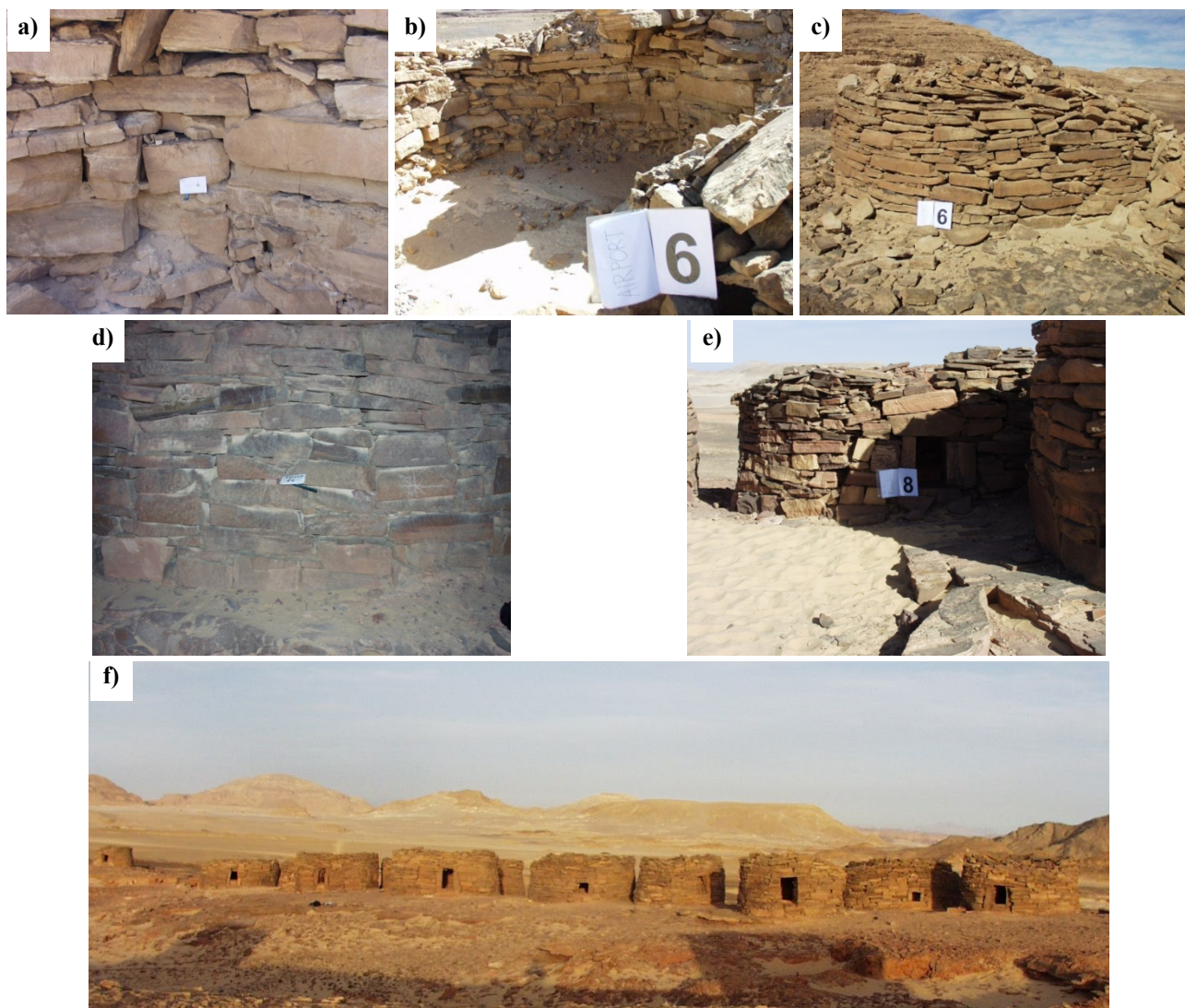


Fig. 3. a) Gebel Gunna No 6. The sampling point (scale of white paper length 20 cm) where piece of slab was taken from inside the tomb, by a hammer and chisel b) another view of the inside with the slabs and rough construction, and c) a view of the back that indicates the construction manner. Height of tombs ~ 2 meters and wall width ~ 1 m (The A4 white paper sheet acts as a scale on the external wall) d) Ain Khodra no 8 sampling from back side, and e) the entrance face (scale as A4 paper and in sampling point paper length is 20 cm) f) also a cluster of tombs around the sampled one.

Dose Rate

U and Th were measured from alphas with the pairs technique by a calibrated alpha counting system; a 7286 Low Level Alpha Counter, Littlemore Sci. Eng Co Oxford with a PM tube type EMI 6097B using ZnS(Ag) films. Alpha counts converted to concentrations and were calibrated on reference standards following devised conversion factors as well as relevant computations (Aitken, 1985; Liritzis and Vafiadou, 2012). Potassium (K%) content was measured by Flame Atomic Absorption Spectroscopy (FAAS) and a minor contribution by Rb to

inclusion from the ratio K_{ppm}/Rb_{ppm} equal 200/1. (Aitken, 1990; Warren, 1978). FAAS was made by Perkin Elmer, USA mod.: Analyst 800 Dual System (Flame and Graphite Furnace ionization). The standard procedure was applied i.e. 0.2 g of sample was transferred to solution in a microwave oven in the presence of 5 ml HF (49%) and 5 ml HNO₃ (69.5%). Thereafter it was diluted to 100 ml. The calibration standard used was SARM 69, from which five solutions of different concentration made the calibration curve. For the conversion from content to dose rate the recent updated factors are used (Liritzis *et al.*, 2013c).

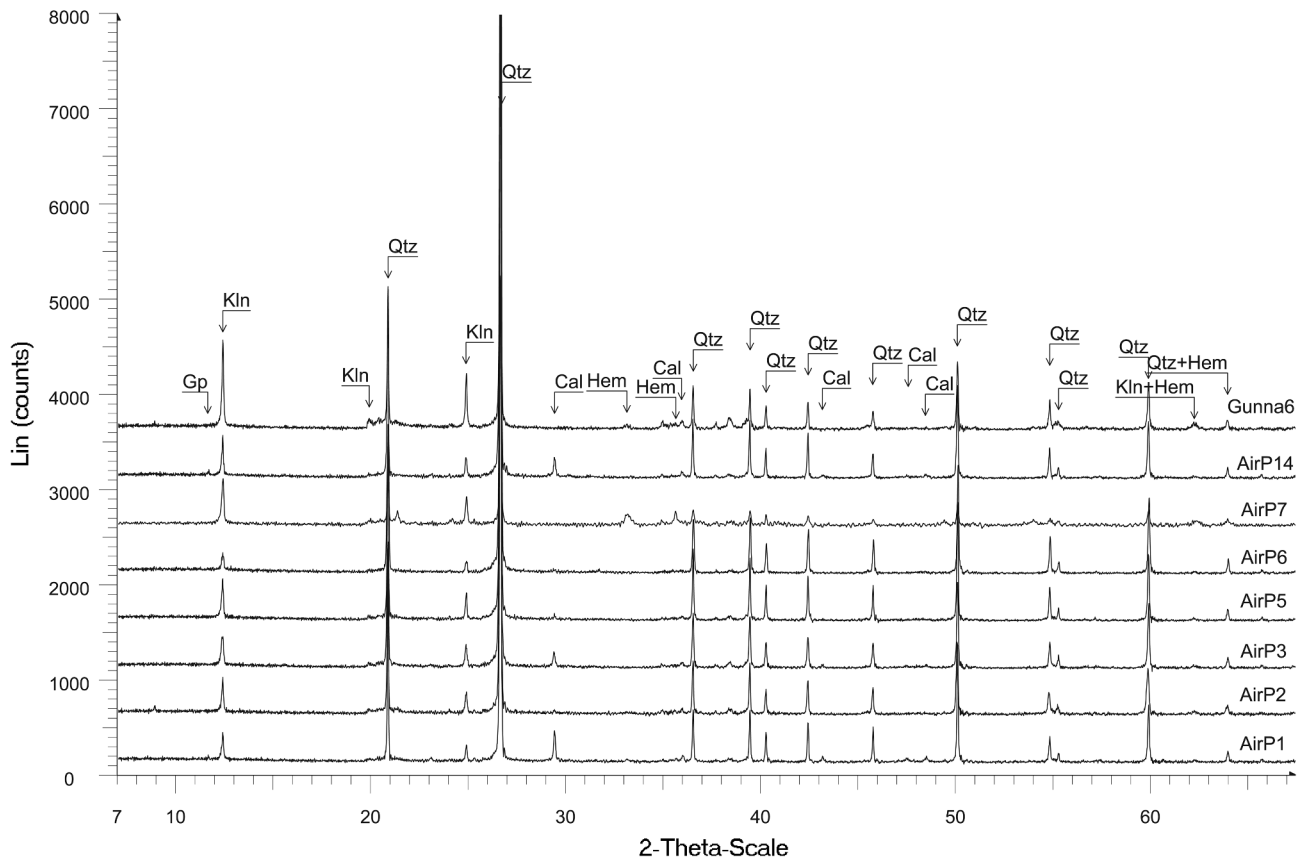


Fig. 4. Composite diagram including the X-ray diffraction patterns of all the samples analysed. Mineral abbreviations are according to Kretz (1983) (main mineral phases Qtz: quartz, Kln: kaolinite, Cal: calcite; Hem: hematite).

The dose rate consists of the sum of beta and gamma dose rates as the outer layer of quartz grains affected by alpha irradiation was removed by acid treatment. However, the sampling position has not a straightforward dosimetry geometry (e.g. sandwiched between sediment layers or sample surrounded by an homogeneous medium in the center of a sphere of radius ~ 35 cm), therefore, dose rates were case sensitive and individually estimated (piece detached from a wall, above a sandy floor *etc.*). Details are given as follows: Rubidium values are calculated based on $K/Rb = 200$. The total beta particle doses-rates are halved (lower stone surface plus upper mortar) and include an attenuation factor of 0.90. For GG6.1 the total D_γ is 1.19 mGy/yr. The D_γ from sand is 1.55 mGy/yr and from stones 0.36 mGy/yr. The sampling point is 60 cm above floor and if considered as a center of a sphere of radius ~ 30 cm (for solid medium, but some meters through air medium) which receives gamma rays dose within 30 cm, including the rock itself, adjoining rocks and mortar, and air from the opposite face of the block: In particular, half gamma dose-rate (equal of 0.180 mGy/yr) from the rear 1 m thick wall and from skyshine inside the enclosed structure of similar stones and the floor, an

approximate 25% ($1/4^{\text{th}}$ of the spherical representation of mixed media around the sampling point) from ground floor sand of 0.39 mGy/yr, plus, 25% from ceiling 0.09 mGy/y. The latter two were estimated from the fact that 70% of infinite gamma dose medium (from K-40, U-238, Th-232) is recorded on surface, and about 25% at a height of 1 meter above ground (Beck and Planque, 1968; Thompson *et al.*, 1999; Liritsiz and Galloway, 1981). For AK8.1.1 the half D_γ dose-rate is used as sample derives from external wall, total D_γ is 1.17 mGy/yr. Water uptake measured to be zero. Cosmic rays dose rate for latitude 28°N and longitude 34°E and altitudes 850–1300 m a.s.l. at Sinai is estimated as 0.30 mGy/yr. The penetration through some centimeters in slabs is estimated to be reduced to 0.25 mGy/yr (Prescott and Hutton, 1994). Total dose rate includes cosmic 0.25 mGy/yr and 0.1 mGy/yr internal radioactivity in quartz.

D_β were contributed to the surface by half from the lower stone where sample powder originates plus half from upper 2 mm layer of sand; from the upper stone surface betas do not reach the lower surface since attenuated by space and introduced sand, while about 20 mi-

crons are removed during cleansing of surface that precludes alpha particles dose.

Equivalent Dose-SAR technique and Resulted Dates

All OSL measurements were conducted in the continuous wave OSL mode of an OSL reader (model Risø TL/OSL – DA15) at 125°C for 100 s. Stimulations were made under blue LEDs light source ($\lambda_p \sim 470$ nm, FWHM 30 nm) and irradiations with a calibrated 0.075 Gy/s $^{90}\text{Sr}/^{90}\text{Y}$ β -ray source (Bøtter-Jensen *et al.*, 2000).

Heating was carried out using a heating rate of 1°C, in order to avoid thermal gradient and 7.5 mm Hoya U-340 ($\lambda_p \sim 340$ nm, FWHM 80 nm) filter for the detection optics. The power level was software controlled and set at 90% of the maximum power of the blue – LED array, delivering at the sample position ~ 32 mW cm⁻². The background OSL levels measured after 95–100 seconds exposure were subtracted from the initial luminescence intensity (0–1 seconds) of the decay curves obtained. The D_e was determined on recovered traces of quartz from sandstones (Liritzis *et al.*, 2010b, 2015, Liritzis and Vafiadou, 2014). OSL signals present an extremely rapid decay in the first seconds of stimulation, providing thus a strong indication regarding the presence of a unique fast component, being dominant at the initial part of the OSL curves. The numbers of aliquots/per sample were very restricted due the nature and the availability of the samples and ranged from 2 to 5; only sample AK8.2.4 provided powder for 7 aliquots (cf. notes on Table 2).

Quartz grain aliquots which were collected in earlier steps during sample preparation (and suspected as being partially or totally bleached) for both samples following SAR, was used to perform initial tests like signal growth, preheat and dose recovery tests and those were 2 aliquots made from sample GG.6.1 and 3 samples made from AK.8.2.4.

Below an OSL shine-down curve is given for an aliquot from sample AK.8.2.4 that was used as a test sample (Fig. 5).

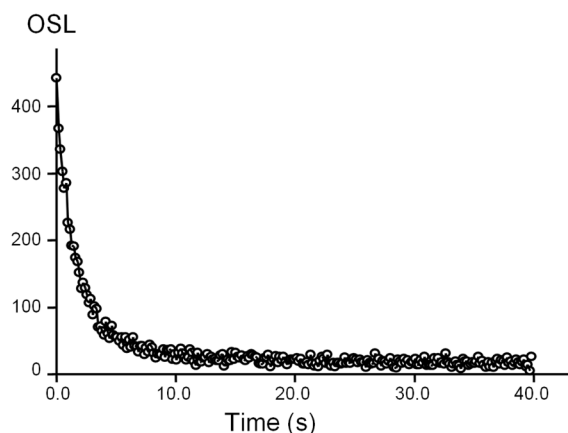


Fig. 5. OSL shine-down curve from sample AK.8.2.4.

Table 2. Luminescence measurements data. (GB: Gebel Gunna, AK: Ain Khodra).

Sample No	U (ppm)	Th (Ppm)	K (%)	Rb (Ppm)	$D\beta$	$D\gamma$	ED ¹ (Gy)	Age (yrs BC)	Annual Dose, (mGy/yr) ²
GG6.1	0.55 ± 0.077	4.97 ± 0.32	0.21 ± 0.008	10.5	0.85 ± 0.1 ³	0.43 ± 0.04 ⁴	4.83 ± 0.33 (3)	1800 ± 320	1.28
GG6.2	>>	>>	>>	>>	>>	>>	5.60 ± 0.45 (5)	2370 ± 300	>>
GG6.3	>>	>>	>>	>>	>>	>>	5.75 ± 0.75 (3)	2490 ± 450	>>
Average								2220 ± 300	
Sand (floor)	4.0 ± 0.09	13.8 ± 1.0	2.50 ± 0.1	123					
AK8.1.1 ⁵	0.89 ± 0.07	2.98 ± 0.23	0.1175 ± 0.005	6	0.20 ± 0.007 ⁶	0.85 ± 0.04	4.89 ± 0.23 (2)	2660 ± 230	1.05
AK8.1.2	>>	>>	>>	>>	>>	>>	4.69 ± 0.35(2)	2470 ± 300	>>
Average								2560 ± 250	
AK8.2.1							3.68 ± 0.35(3)	1500 ± 350	>>
AK8.2.2							3.48 ± 0.23(3)	1310 ± 230	>>
Average								1400 ± 280⁷	
AK8.2.3							4.34 ± 0.40 (5)	2130 ± 370	>>
AK8.2.4							3.13 ± 0.25 (7)	980 ± 240	>>

¹Numbers in brackets in this column indicate number of aliquots measured. The attached errors in all rows were calculated in 1 σ probability; for the errors standard errors given in the ED values, these represent the standard errors of the mean value (e.g. 0.33 for 3 aliquots in samples GG6.1).

²Errors 7–12%.

³Half from lower plus half upper 2 mm layer of sand of 0.58 mGy/yr. Includes internal quartz dose.

⁴For GG6.1 final $D\gamma$ see text, includes cosmic rays dose rate.

⁵For AK8.1.1 sample derives from external wall. 6.

⁶Thickness of sandy powder 3 mm of 0.08 mGy/yr, betas include internal quartz dose.

⁷AK8.2 derives from adjacent slab of AK8.1; Upper slab's surface is AK8.2.1 and 8.2.2; Lower slab's surface is AK8.2.3 and AK8.2.4, not averaged due to large difference.

However, in the sole monolayer aliquots composed by quartz grains resetting of luminescence signal due to solar exposure has been documented, but it is not expected for quartz grains in composite stones likewise sandstones and calcareous schists. Longer sun exposures ensure complete bleaching, in concordance to earlier literature accounts and theoretical considerations of photon attenuation in rocks with depth (Liritsiz and Bakopoulos, 1997, Liritsiz and Galloway, 1999; Habermann *et al.*, 2000; Greilich, 2004; Greilich *et al.*, 2005; Vafiadou *et al.*, 2007; Laskaris and Liritsiz, 2011).

Nine sub-samples were processed derived from three removed stone pieces, two from Ain Khodra and one from Gebel Gunna (Table 2). The flat limited surfaces of the detached pieces which were wrapped in blue opaque bags were divided into regions of interest (ROI) (Fig. 6) where from separate EDs were measured. The latter precaution avoids possible friction which may remove sub areas of the original sun exposed surface. Surface sample was prepared as described above in section 2. All aliquots were checked with infrared (IR) stimulation to ensure the absence of feldspars. The dose recovery test (Fig. 7) varied $\pm 15\%$ around unity and the recycling point around 12% (the dispersed one in GG6.2 given the errors is reasonable; large scatter in the measurement could be due to random error during readouts). A pre-heat test (Fig. 8) provided the 220°C as the suitable to the material temperature threshold.

5. DISCUSSION

The burial structure at Gebel Gunna was amongst a set of six cists built of standing slabs and irregular cobbles, the ground level was sand and skeleton, ribs, other bones and beads were found that date to Late Bronze Age (Bar-Yosef *et al.*, 1983, 1986). According to archaeologists its relationship to the neighboring structures at Gunna area is unclear. Typological examination and radiocarbon dating indicated 3rd millennium BC: for example, the two C-14 ages, at Gunna 25 of 4025 ± 72 BP (SMU-659) and at Gunna 100 of 4373 ± 64 BP (SMU-659) on charcoal from ovens, dug down to bedrock, located in same tomb, cluster but outside the age group of circular tombs (Bar-Yosef *et al.*, 1986). It is worth mentioning the found skeleton of Roman-Byzantine period too. While tombs were used as primary burials, re-use of the structures has been noticed. They were mixed with secondary (later) burials, and/or later historical interventions. This is not surprising because strong stone structures are akin to be reused by later generations. Luminescence dating addresses this as it reinforces an additional value of being applied to reconfirm or question the age of internal findings and its intimate or far relationship with initial construction date.

The estimated ages vary between 1000–2400 BC for the two structures studied, obviously their cluster per sampling point correspond to slightly different ages that fall within the broadly acceptable Bronze Age of the Levant and southern Sinai (Killebrew and Steine, 2014).

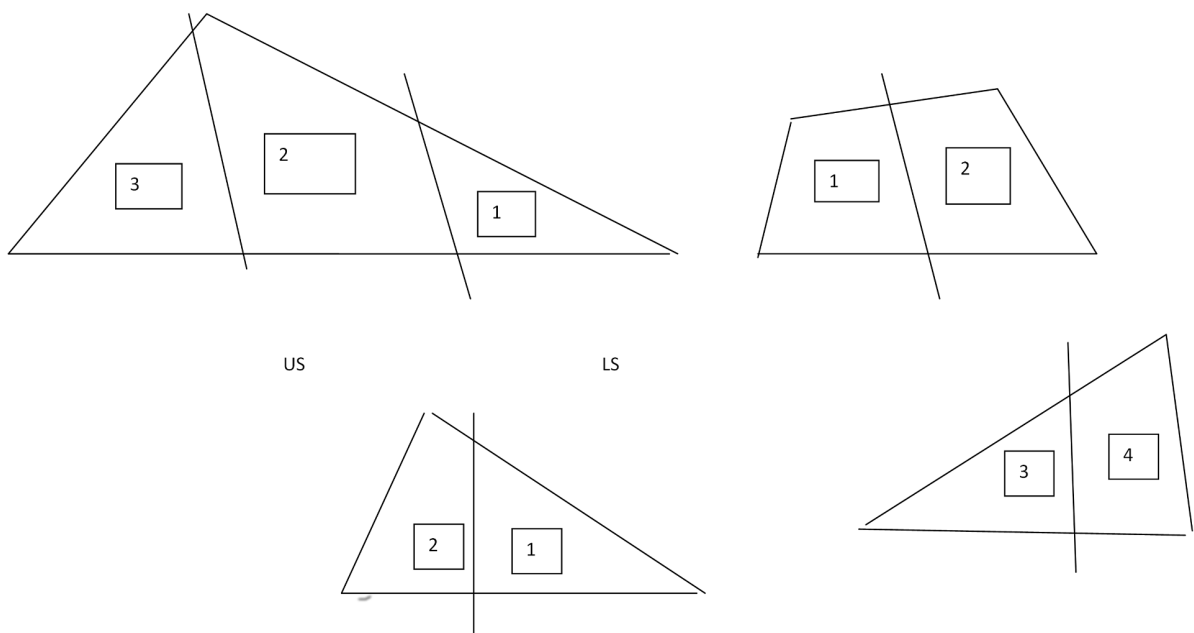


Fig. 6. a) (upper). Sampling three ROI as aliquot powder at a depth of around 1 mm, from Gebel Gunna, (GG6.1, GG6.2, GG6.3), B1) Ain Khodra, AK8.1.1, AK8.1.2; B2) US upper slab's surface (AK8.2.1, 8.2.2) , LS lower slab's surface (AK8.2.3, AK8.2.4).

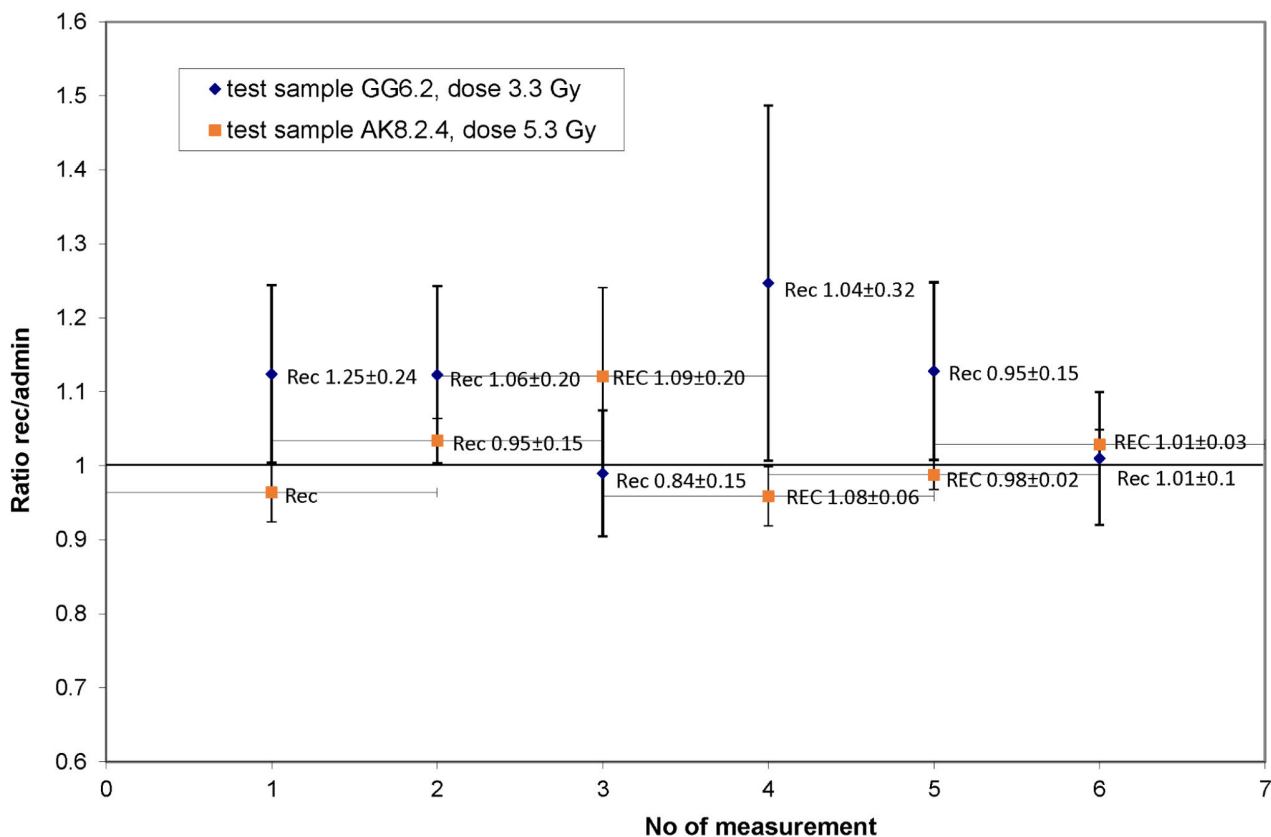


Fig. 7. A multiple dose recovery test (REC numbers) on same 2 aliquots (dose ratio versus the number of measurements): one from sample GG6.2 (diamonds) and one from sample AK8.2.4 (squares). The numbers shown are the ratios measured, together with their errors.

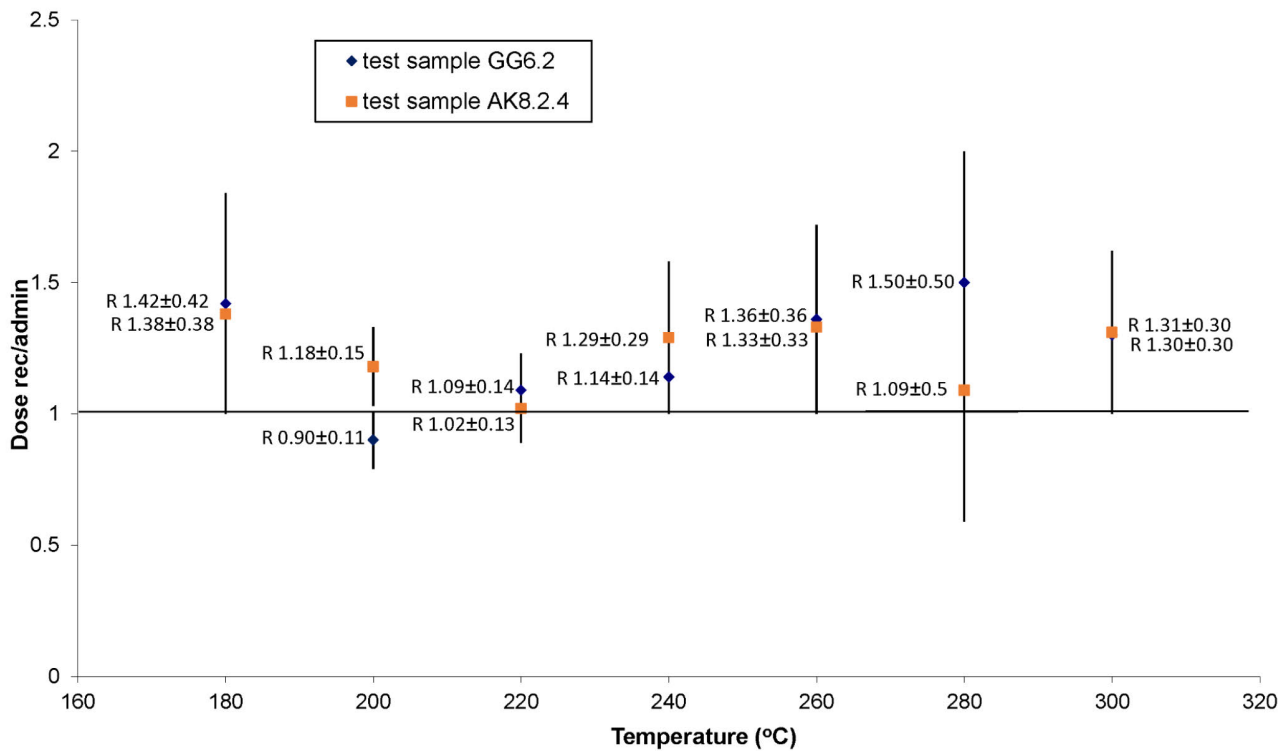


Fig. 8. Pre-heat test using 2 aliquots as in Fig. 6.

For Gebel Gunna (GG6) the average dose from 3 sub-samples provided a highly bracketed dose of 5.13 ± 0.53 Gy which corresponds to an age having as mean value the middle 3rd millennium BC (2220 ± 300 BC) but spanning throughout that Early Bronze Age millennium.

For the Ain Khodra the two samples (AK8.1, AK8.2) derived from the external wall at a height above the external ground approx. 1 meter, and within a 25 cm distance between them. The sample 8.1 gave two similar De and a similar age to Gebel Gunna. The adjacent sample 8.2 consisted of two apparently safe contacts; the upper and lower ones from which four smaller, but one, De were deduced.

The age range of two upper surface slab sub-samples (8.2.1 and 8.2.2) from Ain Khodra falls within the 2nd half of 2nd millennium BC and those lower surface of same slab sub-samples (8.2.3 and 8.2.4) of 2130 BC and 980 BC respectively not averaged due to large difference (see Footnote 7 in **Table 2**).

Obviously the latter apparent unconformity can be attributed either to later building activities of this part or partial exposure to sunlight. However, the Late Bronze Age presence in Gebel Gunna tombs documented by Bar-Yosef *et al.* (1986) is also supported by present OSL results.

6. CONCLUSION

The dating of two *Nawamis* tombs from two *Nawamis* fields in southern Sinai, Gebel Gunna and Ain Khodra, were re-examined, by applying for first time the surface luminescence dating. The standard procedure of sampling for surface luminescence dating of buildings was used, the SAR protocol was employed for ED estimation, and dose rate in mixed radiation field was properly evaluated. Total bleaching is assumed for the upper millimeter surface layer. OSL ages have been derived from nine sub samples of two tombs from Gebel Gunna and Ain Khodra.

Satisfactory criteria tests applied sway opinion that the calculated dates obtained correspond to Levant and southern Sinai archaeological phases of Early Bronze ages with presence of three dates at later Late Bronze period. Archaeological rescue excavation and C14 ages on charcoal from similar tombs as well as detailed typological analysis on plethora of tools indicated an Early Bronze age with some presence at later period.

ACKNOWLEDGEMENTS

Ioannis Liritzis and Fahad Al-Otaibi thank the Dean-ship of Scientific Research at King Saud University for funding the execution of work through the research group project No. RGP-VPP-194. IL also thanks Flora Vafea, father Daniel and sister Styliani for their help during one fieldwork season, Archbishop of St Catherine's Monas-

tery at Sina Rev.Damianos and the priesthood for their hospitality, Prof.Ashok Sinhgvi for useful comment, and the Supreme Council of Antiquities of Egypt for permission that took place during fieldwork the south of Sinai during June 2006 for the work on Sarabet El-Khadem Temple, made under the supervision of co-author Prof. Mosalam Shaltout in June 2006, Chairman of the mission of Archaeoastronomy in the Ancient Egypt. We thank the two anonymous reviewers for constructive comments.

REFERENCES

- Aitken MJ, 1990. *Science-Based Dating in Archaeology*. Addison Wesley Longman Ltd, London
- Aitken MJ, 1985. *Thermoluminescence Dating*, Academic Press, London.
- Bar-Yosef O, Belfer-Cohen A, Goren A, Hershkovitz I, Ilan O, Mienis HK and Sass B, 1986. *Nawamis* and habitation sites near Gebel Gunna, southern Sinai. *Israel Exploration Journal* 36: 121–167.
- Bar-Yosef O, Belfer-Cohen A, Goren A and Smith P, 1977.. The *nawamis* near 'Ein Huderah (eastern Sinai). *Israel Exploration Journal* 27: 65–88.
- Bar-Yosef O, Hershkovitz I, Arbel G and Goren A, 1983.. The orientation of *nawamis* entrances in southern Sinai: expressions of religious belief and seasonality? *Tel Aviv* 10: 52–60.
- Beck H and de Planque G, 1968. The radiation field in air due to distributed gamma-ray sources in the ground. United States Atomic Energy Commission, Division of Technical Information, HASL-195, U.S Dept of Commerce, Springfield, Virginia, 22151.
- Botter-Jensen L, Solongo S, Murray AS, Banerjee D and Jungner H, 2000. Using the OSL single-aliquot regenerative-dose protocol with quartz extracted from building materials in retrospective dosimetry. *Radiation Measurements* 32: 841–845, DOI 10.1016/S1350-4487(99)00278-4.
- Greulich S, Glasmacher GA and Wagner GA, 2005. Optical dating of granitic stone surfaces. *Archaeometry* 47(3): 645–665, 10.1111/j.1475-4754.2005.00224.x.
- Greulich S, 2004. Über die Datierung von Gesteinsoberflächen mittels optisch stimulierter Lumineszenz (On the dating of rock surfaces by means of optically stimulated luminescence). Ph.D Dissertation, University of Heidelberg.
- Habermann J, Schilles T, Kalchgruber R and Wagner GA, 2000. Steps towards surface dating using luminescence. *Radiation Measurements* 32: 847–851, DOI 10.1016/S1350-4487(00)00066-4.
- Hershkovitz I, Arbel G, Bar-Yosef O and Goren A, 1985.. The relationship between *nawamis* entrance orientations and sunset direction. *Tel Aviv* 12: 205–211.
- Huntley DJ and Richards MP, 1997. The age of the Diring Yuriakh archaeological site. *Ancient TL* 15(2–3): 48–49.
- Iliopoulos I, Xanthopoulou V and Tsolis-Katagas P, 2011. *A petrographic assessment of houseware and storage pithoi in the Early Helladic settlement of Helike, Achaia, Greece*. In: D. Katsonopoulou (ed.) *Helike IV, Protohelladika: Helike and Aigialeia, The Southern Greek Mainland*, pp. 127–142.
- Killebrew AE and Steiner M eds, 2014. *The Oxford Handbook of the Archaeology of the Levant: c. 8000–332 BCE*, Oxford Handbooks in Archaeology, OUP, Oxford, UK, DOI: 10.1093/oxfordhb/9780199212972.001.0001.
- Kretz R, 1983. Symbols for rock-forming minerals. *American Mineralogist* 68: 277–279.
- Laskaris N and Liritzis I, 2011. A new mathematical approximation of sunlight attenuation in rocks for surface luminescence dating. *Journal of Luminescence* 131: 1874–1884, DOI 10.1016/j.jlumin.2011.04.052.
- Liritzis I and Galloway RB, 1981. Correlation of variations in the gamma-ray dose-rate in soil with meteorological factors. *Archaeometry* 23(1): 109–113, DOI 10.1111/j.1475-4754.1981.tb00961.x.

- Liritzis I, 1994. A new dating method by thermoluminescence of carved megalithic stone building. *Comptes Rendus Academie des Sciences serie II* 319: 603–610.
- Liritzis I and Bakopoulos Y, 1997. Functional behaviour of solar bleached thermoluminescence in calcites. *Nuclear Instruments and Methods B* 132: 87–92, DOI 10.1016/S0168-583X(97)00380-7.
- Liritzis I and Galloway RB, 1999. Dating implications from solar bleaching of thermoluminescence of ancient marble. *Journal Of Radioanalytical And Nuclear Chemistry* 241(2): 361–368, DOI 10.1007/BF02347476.
- Liritzis I, Polymeris G and Zacharias N, 2010. Surface luminescence dating of ‘Dragon Houses’ and Armena Gate at Styra (Euboea, Greece). *Mediterranean Archaeology and Archaeometry, Special Issue* 10(3): 65–81.
- Liritzis I, 2010. Strofilas (Andros Island, Greece): New evidence of Cycladic Final Neolithic dated by novel luminescence and Obsidian Hydration methods. *Journal of Archaeological Science* 37: 1367–1377, DOI 10.1016/j.jas.2009.12.041
- Liritzis I, 2011. Surface dating by luminescence: An Overview. *Geochronometria* 38(3): 292–302, DOI 10.2478/s13386-011-0032-7.
- Liritzis I and Vafiadou A, 2012. Calibration aspects of thick source alpha counter ZnS system. *Measurement* 45: 1966–1980, DOI 10.1016/j.measurement.2012.04.026.
- Liritzis I and Vafiadou A, 2014. Surface luminescence dating of some Egyptian monuments. *Journal of Cultural Heritage* 16: 134–150, DOI 10.1016/j.culher.2014.05.007.
- Liritzis I, Singhvi AK, Feathers JK, Wagner GA, Kadereit A, Zacharias N and Li S-H, 2013a. Luminescence Dating in Archaeology, Anthropology and Geoarchaeology: An Overview. Springer Briefs in Earth System Sciences, DOI 10.1007/978-3-319-00170-8
- Liritzis I, Vafiadou A, Zacharias N, Polymeris GS and Bednarik RG, 2013b. Advances in surface luminescence dating: some new data from three selected Mediterranean sites. *Mediterranean Archaeology & Archaeometry* 13(3): 105–115.
- Liritzis I, Stamoulis K, Papachristodoulou Ch and Ioannides KG, 2013c. A re-evaluation of radiation dose rate conversion factors. *Mediterranean Archaeology & Archaeometry* 13(3): 1–15.
- Liritzis I, Aravantinos V, Polymeris GS, Zacharias N, Fappas I, Agiamarniotis G, Sfampa IK, Vafiadou A and Kitis G, 2015. Witnessing prehistoric Delphi by Luminescence dating. *Comptes Rendus Palevol* 14: 219–232, DOI 10.1016/j.crpv.2014.12.007.
- Morgenstein ME, Luo S, Ku TL and Feathers J, 2003. Uranium series and luminescence dating of volcanic lithic artefacts. *Archaeometry* 45(3): 503–518, DOI 10.1111/1475-4754.00124.
- Murray AS and Wintle AG, 2000. Luminescence dating of quartz using an improved single-aliquot regenerative-dose protocol. *Radiation Measurements* 32: 57–73, DOI 10.1016/S1350-4487(99)00253-X.
- Prescott JR and Hutton JT, 1994. Cosmic ray contributions to dose rates for luminescence and ESR dating: Large depths and long-term variations. *Radiation Measurements* 23: 497–500, DOI 10.1016/1350-4487(94)90086-8.
- Roberts RG, Jacobs Z, Bo Li, Jankowski NR, Cunningham AC, Rosenfeld AB, 2015. Optical dating in archaeology: thirty years in retrospect and grand challenges for the future. *Journal of Archaeological Science* 56: 41–60, DOI 10.1016/j.jas.2015.02.028.
- Sohbati R, 2013. *Luminescence, Rock Surfaces*. Encyclopedia of Scientific Dating Methods, Springer Science+Business Media Dordrecht 2013, p. 1–7, DOI 10.1007/978-94-007-6326-5_83-4.
- Thompson IMG, Botter-Jensen L, Deme S, Pernicka F, Saez-Vergara JC, eds, 1999. EURADOS Working Group 12 “Environmental Radiation Monitoring”, Technical recommendations on measurements of external environmental gamma radiation field. Radiation Protection 106. European Commission. Luxembourg ISBN 92-828-7811-2, 177 p.
- Vafiadou A, Murray AS and Liritzis I, 2007. Optically Stimulated Luminescence (OSL) dating investigations of rock and underlying soil from three case studies. *Journal of Archaeological Science* 34: 1659–1669, DOI 10.1016/j.jas.2006.12.004.
- Warren SE, 1978. Thermoluminescence dating of pottery - an assessment of the dose-rate from rubidium. *Archaeometry* 20(1): 71–72, DOI 10.1111/j.1475-4754.1978.tb00215.x.
- Wanas HA, 2011. The Lower Paleozoic rock units in Egypt: An overview. *Geoscience Frontiers* 2(4): 491–507, DOI 10.1016/j.gsf.2011.06.004.